The Astrophysical Journal, 494:799–805, 1998 February 20
© 1998. The American Astronomical Society. All rights reserved. Printed in U.S.A.

OUTMOVING CLUMPS IN THE WIND OF THE HOT O SUPERGIANT ζ PUPPIS

Thomas Eversberg,[1] Sébastien Lépine,[1] and Anthony F. J. Moffat[1]
Département de Physique, Université de Montréal, C.P. 6128, Succ. Centre Ville, Montréal H3C 3J7, Canada; Observatoire du Mont Mégantic;
eversberg@astro.umontreal.ca
Received 1997 February 6; accepted 1997 September 30

ABSTRACT

We present time series of ultra–high S/N, high-resolution spectra of the He II 4686 Å emission line in the O4I(n)f supergiant ζ Puppis, the brightest early-type O star in the sky. These reveal stochastic variable substructures in the line, which tend to move away from the line center with time. Similar scaled-up features are well established in the strong winds of Wolf-Rayet stars (the presumed descendants of O stars), where they are explained by outward-moving inhomogeneities (e.g., blobs, clumps, and shocks) in the winds. If all hot star winds are clumped like that of ζ Pup, as is plausible, then mass loss rates based on recombination-line intensities will have to be revised downward. Using a standard "β" velocity law, we deduce a value of $\beta = 1.0$–1.2 to account for the kinematics of these structures in the wind of ζ Pup. In addition to the small-scale stochastic variations, we also find a slow systematic variation of the mean central absorption reversal.

Subject headings: line: profiles — stars: early-type — stars: individual (ζ Puppis) — stars: mass loss — supergiants

1. INTRODUCTION

The most massive stable stars known have O-type spectra. Among the O stars, the hotter ones tend to have the highest masses. Coupled with this high mass is a high luminosity (and high surface temperature), which drives a strong wind and leads to various kinds of instability and variability, such as blue-to-red moving substructures in photospheric absorption lines associated with surface nonradial pulsations (NRP; e.g., Baade 1988), and red-to-blue propagating discrete absorption components (DAC; e.g., Prinja & Howarth 1986) in the absorption edges of strong P Cygni lines, probably associated with corotating interacting regions (CIR; e.g., Cranmer & Owocki 1996). Conversely, study of the variability can provide useful constraints on the nature of massive stars and their strong winds.

Although O stars are very rare, compared to lower mass stars, their extremely bright intrinsic luminosity makes them appear significant in number among the apparently brightest stars in the sky. The brightest *early-type* O star in the sky is the second visual magnitude O4I(n)f star ζ Puppis. Its variability has therefore been scrutinized considerably in the past. As it turns out, ζ Pup manifests a high degree of variability, compared to other bright single O stars, probably because of its large $v \sin i$ for a supergiant of 220 km s^{-1} (Prinja 1988; Kaper et al. 1996). This high rotation velocity may be related to its runaway status (Blaauw 1993). In Table 1 we summarize some major properties of ζ Pup (see also Reid & Howarth 1996).

In particular, ζ Pup shows three distinct timescales in its variability:

1. $P_1 = 5.1 \pm 0.1$ days, seen in Hα (e.g., Moffat & Michaud 1981; Ebbets 1982), UV P Cygni lines (e.g., Prinja 1992; Howarth, Prinja, & Massa 1995), and X-rays (Berghöfer et al. 1996a). This is likely the rotation period, with $\sin i$ close to unity (Reid & Howarth 1996).

2. $P_2 = 15$–19 hr, seen in Hα and UV wind lines (Prinja 1992; Howarth et al. 1995; Reid & Howarth 1996). This is the recurrence timescale of DACs; it is not strictly periodic. Even the 16.7 ± 0.8 hr periodicity found (simultaneously with Hα) in moderately high-energy X-rays by Berghöfer et al. (1996a) probably falls in this category.

3. $P_3 = 8.54 \pm 0.05$ hr, found in blue-to-red moving bumps on photospheric absorption lines (Baade 1986, 1988; Reid & Howarth 1996). This period is probably the result of NRP in the stellar surface, with $l = -m = 2$. Higher modes ($-m = 4$, 8) have been seen only on one occasion (Baade 1991). Whether P_3 is fundamentally related to P_2, e.g., a harmonic with $P_3 = \bar{P}_2/2$, remains to be settled. Also, with the data available presently, it is still not established whether or not $\bar{P}_2$ is a simple fraction (e.g., $\frac{1}{6}$) of the rotation period P_1, as expected for fixed perturbations on the rotating stellar surface. A possible connection between rapid rotation and DAC activity arises in the spectropolarimetric evidence for an aspherical wind in ζ Pup (Harries & Howarth 1996).

Another type of variability in hot stars, stochastic variability, has so far only been seen clearly and directly in stars with very strong winds. The intense winds of Wolf-Rayet (W-R) stars (the descendants of O stars) exhibit small-scale variations in their (more easily observed) optical emission lines (Robert 1992; Moffat & Robert 1992). These are believed to arise in density perturbations (clumps) throughout the W-R wind, as a result of supersonic compressible turbulence (Henriksen 1994) driven by radiative instabilities (Owocki 1994; cf. Chiueh 1997 for an alternative explanation). Indirect evidence for clumpy structure in O star winds has been proposed, e.g., via X-ray observations (Chlebowski, Harnder, & Sciortino 1989; Hillier et al. 1993), although no stochastic X-ray variation has been seen clearly yet (Berghöfer, Schmitt, & Cassinelli 1996b). Hillier et al. (1993) modeled the 0.1–2.5 keV spectrum of ζ Pup under the assumption that turbulence and associated shocks in the wind are the origin of the observed X-ray flux. Their results are supported by more recent calculations of Feldmeier et al. (1997).

[1] Visiting Astronomer, Canada-France-Hawaii Telescope, operated by the National Research Council of Canada, the Centre National de la Recherche Scientifique de France, and the University of Hawaii.

TABLE 1

Observed Properties of ζ Pup

Property	Value	References
Spectral Type	O4I(n)f	1
V (mag)	2.26	2
T_{eff}(kK)	42.0	3, 4, 5
$R_*/R_\odot$	$18.4^{+5.2}_{-3.3}$	4
$M_*/M_\odot$	52.5	5
$\log \dot{M}$ ($M_\odot$ yr^{-1})......	-5.57 ± 0.15	6
v_∞ (km s^{-1})...........	2250	5
$v \sin i$ (km s^{-1})........	220	5
d (pc)	429^{+120}_{-77}	6, 7

References.—(1) Walborn 1972; (2) Johnson 1965; (3) Bohannan et al. 1986; (4) Kudritzki et al. 1983; (5) Puls et al. 1996; (6) Schaerer, Schmutz, & Grenon 1997; and (7) van der Hucht et al. 1997.

A key question here concerning the lack of direct detection of such perturbations in O star winds heretofore is whether such perturbations simply do not arise in O star winds, or whether the observed wind lines in O stars are so weak that their detection has been difficult. ζ Pup is an obvious first target for this purpose, since it has a relatively strong wind for an O star, and it is very bright, allowing one to obtain very high-quality spectra in a short time. In this paper, we attempt to answer this question.

2. OBSERVATIONS AND DATA REDUCTION

Observations of ζ Pup were made at the f/8.2 coudé focus of the 3.6 m Canada-France-Hawaii Telescope (CFHT) for ~5 hr during the nights of 1995 December 10/11 and 12/13. Using the red coudé train and image slicer, the 1800 line mm^{-1} holographic grating, and the Reticon 1872 array as a detector (see the CFHT User's Manual, and references therein), we obtained S/N ≈ 1000/0.03 Å pixel in 10 minutes on a total range of 60 Å centered on He II 4686 Å. Along with Hα, this is the strongest wind line in the optical spectrum of ζ Pup. However, He II has the advantage both of forming close to the star *and* of being much less affected by variable telluric features. The Reticon uses four amplifiers, one for every fourth pixel. Their different sensitivities cancel out through flat-fielding. The data reduction was carried out using IRAF with a Reticon reduction package developed by D. Bohlender and G. Hill, which includes the baseline reduction, flat fielding, heliocentric correction, and wavelength calibration with a Thorium-Argon comparison spectrum. The FWHM of the Th-Ar lines covers ~2 pixels, and the wavelength shift over each night was negligibly small. The 60 Å window is too small to cover the whole He II emission line, and its blue wing is affected by the N III emission-line complex. To obtain a reasonable and repro-

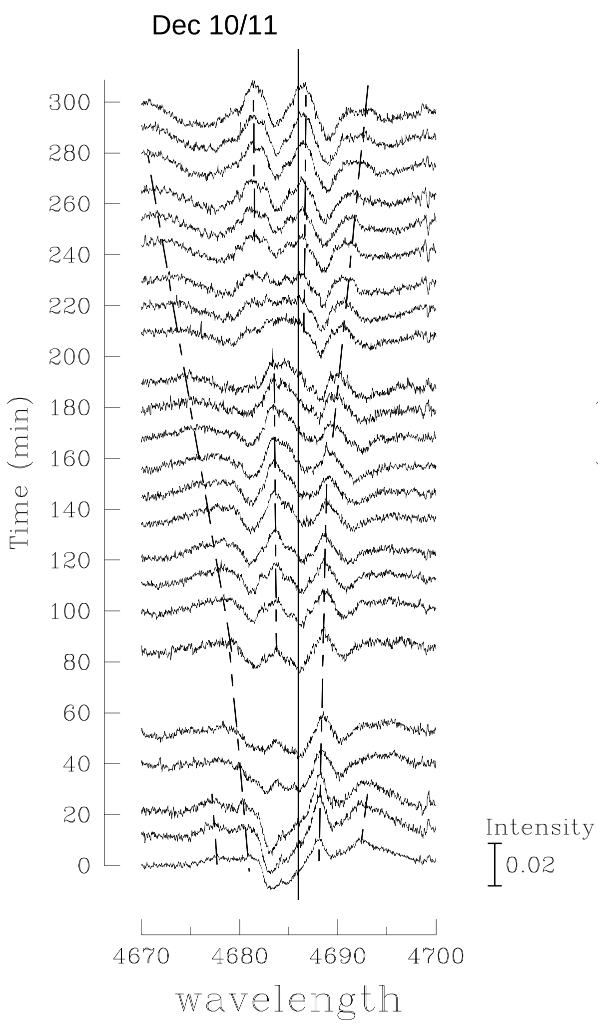

Fig. 1.—Residuals of He II 4686 for ζ Pup on 1995 December 10/11 and 12/13. The vertical axis gives the intensity and the time, respectively. The scale for the residual intensities is indicated. Dashed lines trace detected variations during the night. Vertical solid lines indicate the rest wavelength.

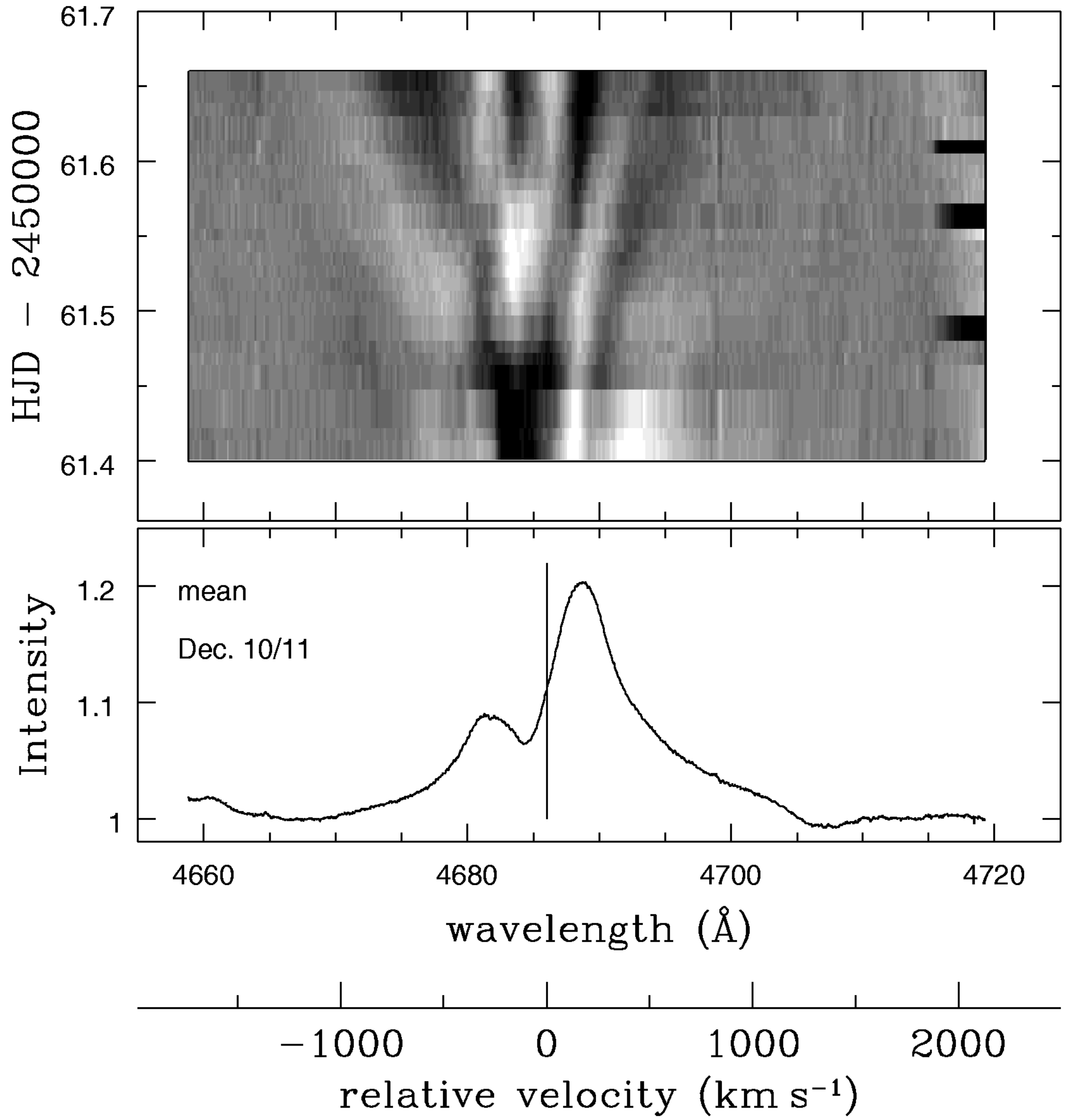

FIG. 2.—Observed He II 4686 spectra of ζ Pup for the night of 1995 December 10/11. *Top:* Gray-scale plot of nightly residuals from the mean rectified spectrum of each night plotted in time (stretched appropriately to fill in time gaps) vs. wavelength. *Bottom:* Mean spectrum. The vertical line corresponds to the rest wavelength (4685.73 Å), not allowing for any peculiar motion of the star.

ducible quasi-continuum, we have fitted a straight line through two ranges of 1 Å ($\approx$30 pixels) in the extreme blue/red wings for each spectrum at the same position. This was divided into each spectrum to produce quasi-rectified emission profiles.

3. RESULTS AND DISCUSSION

3.1. *Small-Scale Variations*

As a first step we have co-added all spectra to yield a mean for each night. This was then subtracted from the individual spectra. The resulting plots are shown in Figure 1. The respective gray-scale plots and the nightly means are shown in Figures 2 and 3.

A first look at the gray-scale plots in Figures 2 and 3 shows that individual residual emission features move away from line center to the blue/red wing of the line. All features tend to smear out with time, while the intensity first rises, then drops. In order to explore the global variability, we first calculated the standard deviation of pixel i,

$$\sigma_i = \left[\frac{1}{n-1}\sum_{j=1}^{n}(I_{ij} - \bar{I}_i)^2\right]^{1/2} , \qquad (1)$$

where I_{ij} is the rectified intensity of pixel i of the jth spectrum, and $\bar{I}_i$ is the mean rectified spectrum at pixel i. The results for both nights are shown in Figures 4 and 5. Allowing for statistical fluctuations, the variation profile across the line, $\sigma(\lambda)$, follows the same basic shape of the line profile $I(\lambda)$ itself, with $\sigma(\lambda)/I(\lambda) \sim 5\%$ and a small systematic increase in $\sigma(\lambda)$ on the blue side of the line, where a small level of P Cygni absorption likely prevails. This implies that wind variations occur *throughout* the wind where He II 4686 is emitted. These short-term variations in emission-line profile appear to occur without any noticeable influence from the near-central absorption reversal.

To consider the line variability in more detail, we traced the radial velocities of individual subpeaks with time (see Fig. 1). This was often a delicate operation: the He II line has a peak intensity of only 1.2 × continuum (compared to several times the continua in W-R lines), and the residuals are still relatively noisy. The form of single features can

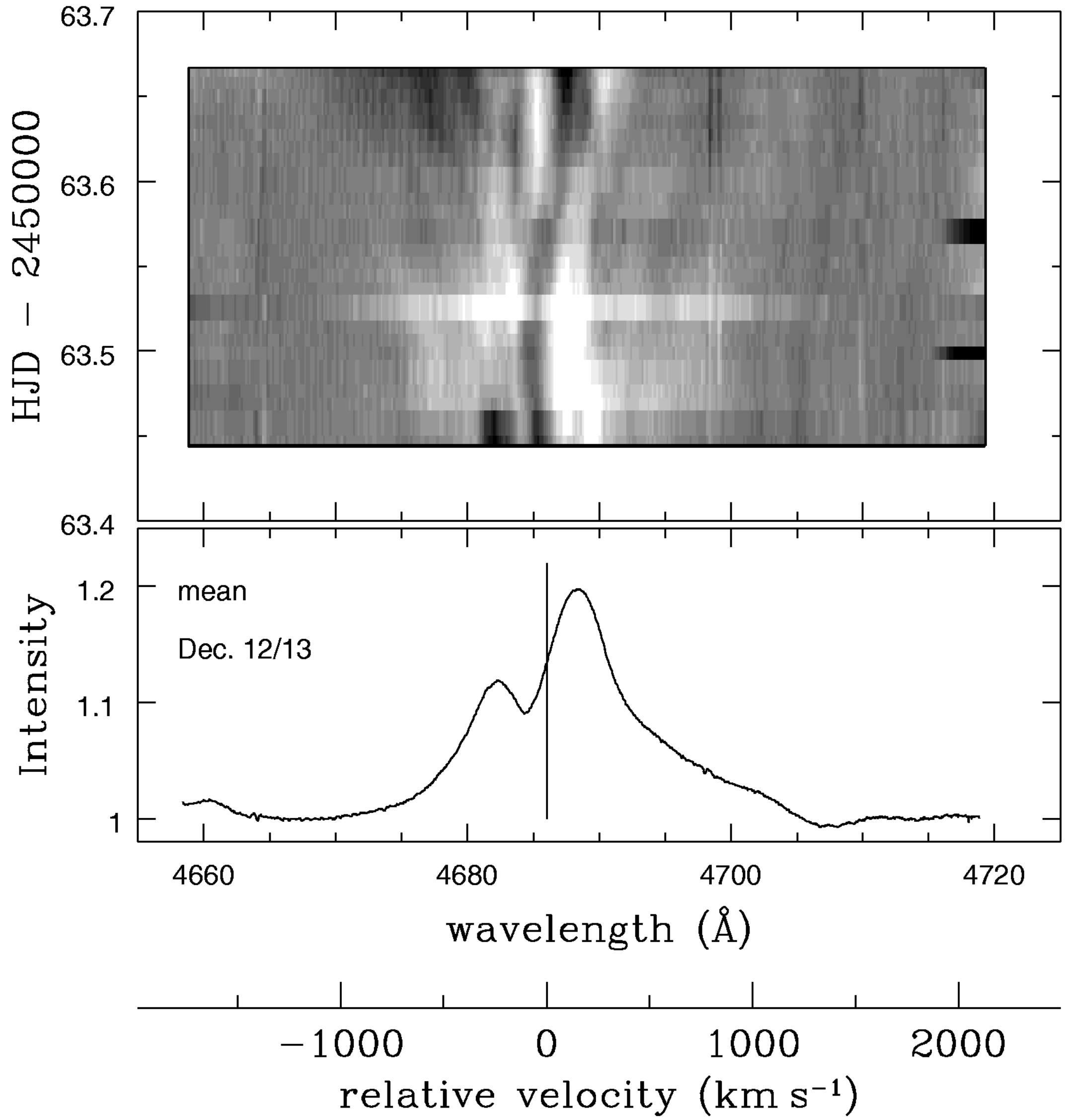

FIG. 3.—Same as in Fig. 2, but for 1995 December 12/13

change very quickly from one spectrum to the next, e.g., from Gaussian-like forms to double-peaked triangles. We therefore assume that the nonsimple form of even the most obvious subfeatures may be the result of blends of many unresolved features. After trying unsuccessfully to de-blend the subpeaks with multi-Gaussian fits and simple peak measurements, we decided to keep things as simple as possible by fitting single Gaussians only to the most prominent features. On the other hand, this assumption for the sake of simplicity and consistency also means that we will be clearly limited in detecting a relatively small number of blobs.

Does a β velocity law fit the observed trajectories? We attempt to answer this by looking at the detailed motion of the clearest, most prominent traced subpeak, visible on the near red side of the line center of He II 4686 during the whole observing sequence of 1995 Dec 10/11 (see Fig. 2). Figure 6 shows a plot of observed velocity versus time for this feature, which actually consists of two distinct branches. Superposed on these data are theoretical β-laws, obtained using $v(r) \equiv dr/dt = v_\infty(1 - R_*/r)^\beta$, converted to $v(t)$[2] and then to projected velocity $V(t) \equiv v(t) \cos \theta$, for different values of β and θ (the assumed constant angle between blob trajectory and the line of sight). The first branch (*open circles*) can be matched by a β-law with $1 < \beta \lesssim 2$ (and $100° < \theta \lesssim 140°$, respectively), while the second branch (*filled circles*) requires $1 \lesssim \beta \ll 2$ ($112° \lesssim \theta \ll 180°$). If the clumps follow a unique β-law, these two branches taken together suggest $1 < \beta < 2$. In comparison, Reid & Howarth (1996) obtained $\beta \approx 1$, using the same technique for variations with longer time coverage on the blue side of the Hα wind line of ζ Pup.

All traced structures show nearly linear propagation with time. This may seem curious, considering the standard velocity law with *nonlinear* behavior. However, the blobs have been traced over only a relatively small range in distance, so that linear motion is a good approximation. Then, it is possible to characterize the blob trajectories by a mean acceleration and velocity in the observer's frame, and to compare all observed blobs with the velocity law for fixed β but different θ (see also Moffat & Robert 1992). The results

[2] From $v_\infty t = \text{constant} + \int dr/(1 - R_*/r)^\beta$.

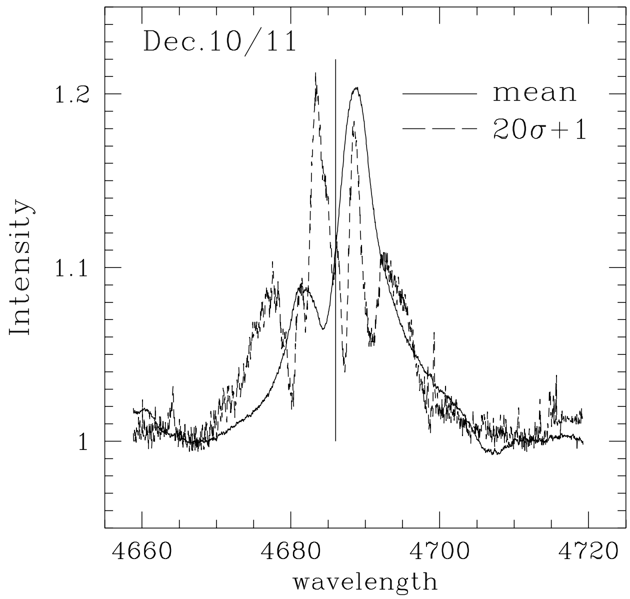

FIG. 4.—Mean rectified spectrum (*solid line*) and standard deviation σ (*dashed line*) for December 10/11. The σ profile is expanded by a factor of 20 and increased by 1.0 in intensity in order to match the mean rectified line profile as closely as possible.

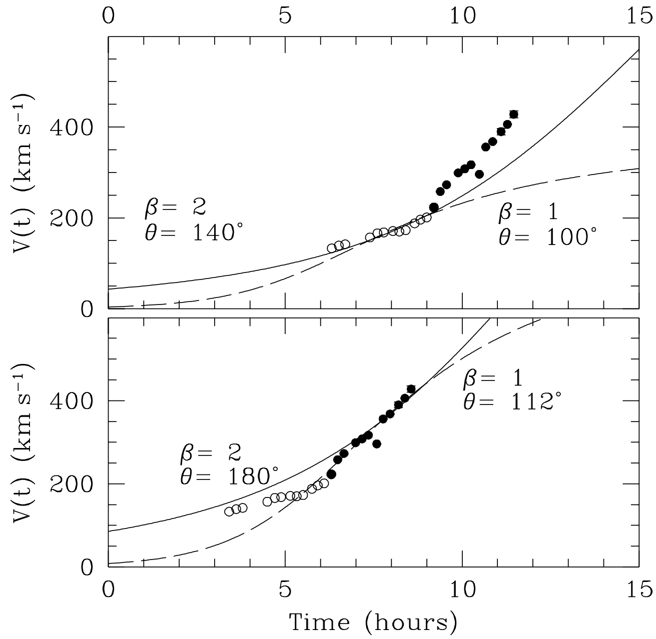

FIG. 6.—Projected velocity vs. time of the most clearly identified and traced subpeak in the wind of ζ Pup, on 1995 December 10/11 at $V(t) \sim 130$–450 km s^{-1} (see Fig. 2). This subpeak actually consists of two distinct clumps indicated by different symbols. The transition point from one clump to the other is somewhat subjective. Error bars are indicated or are smaller than the data points. Sample lines represent the standard velocity law matched to each clump for pairs of β and θ. The origin on the time axis was arbitrarily chosen to occur when $v = 0.01v_\infty$ for the $\beta = 1$ curves.

are shown in Figures 7 and 8, where we explore which values of β and R_* allow one to fill in the areas of permitted substructures best, assuming that they propagate like a single β-law wind. It would appear that the standard $\beta = 0.8$ law for O star winds (Pauldrach, Puls, & Kudritzki 1986) does not do this best, at least for clumps, with a dearth of features for $|\dot{V}| \gtrsim 0.05$ km s^{-2}, where, if any features existed, they should be seen. On the other hand, a value of $\beta \approx 1.1$ does a better overall job. We claim that a value of β in the range ≈ 1.0–1.2 best satisfies the data in Figures 7 and 8. Such a range is also compatible with the detailed trajectories in Figure 6. Figures 7 and 8 show also that most observed substructures are found at $R \lesssim 2R_*$ (*solid trajectories*), with a preference at $R \lesssim 1.5R_*$ for the most accelerated features.

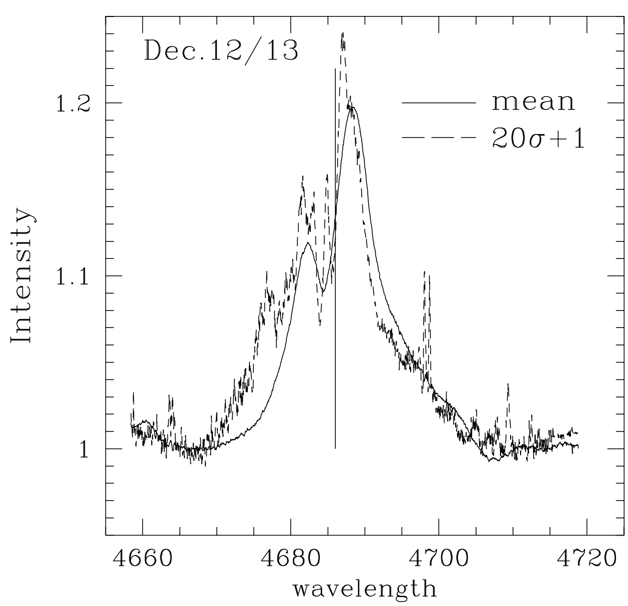

FIG. 5.—Same as Fig. 4, but for December 12/13

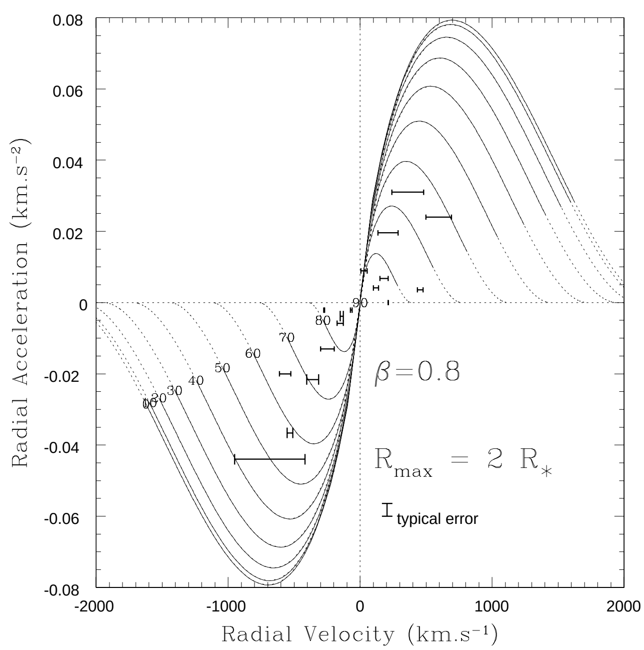

FIG. 7.—Plot of (projected) radial acceleration $\dot{V}$ vs. radial velocity V for individual blobs in He II 4686. Each curve represents a locus with respect to the line of sight from $\theta = 0°$ (*lower curve*) to $\theta = 180°$ (*upper curve*). Model loci are based on $V = v(r) \cos \theta$ and $v(r) = v_\infty(1 - R_*/r)^\beta$ for $\beta = 0.8$ (the standard value for OB star winds). Solid lines are extended by dotted lines that go beyond R_{max}. The adopted terminal velocity is $v_\infty =$ 2250 km s^{-1}, and the adopted stellar radius is $R_* = 18R_\odot$. Horizontal bars indicate the velocity range of an identified and traced substructure. The rms error (1 σ) for the acceleration is indicated.

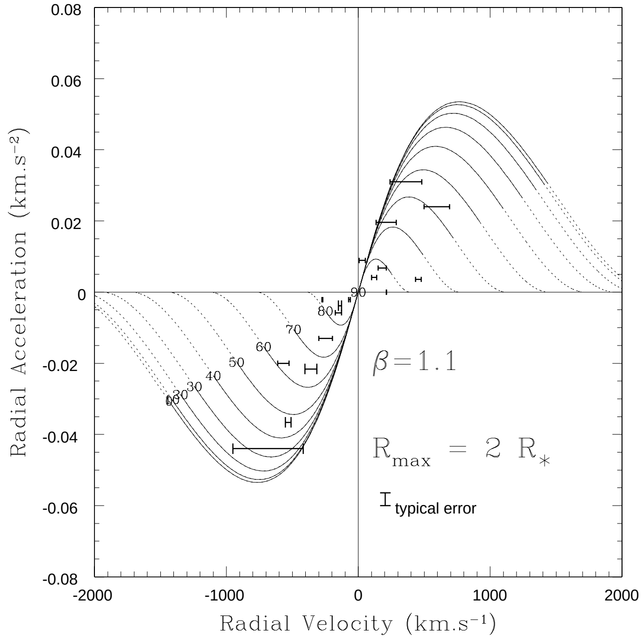

FIG. 8.—Same as Fig. 7, but for $\beta = 1.1$

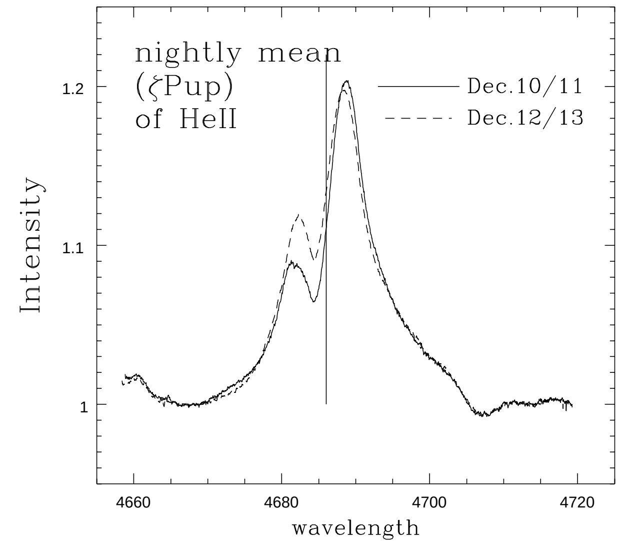

FIG. 9.—Nightly mean of December 10/11 (*solid line*), compared to December 12/13 (*dashed line*).

Note that on the blue side, accelerations are detected that reach higher values than on the red side. This could result from small number statistics (we detected only 17 features). On the other hand, it could be that features in the red at large projection angles and close to the star are hidden by the star itself, so that we are seeing the manifestation of a *shadow effect*.

Do the substructures in Figures 7 and 8 appear randomly in time? With only 5 hr coverage each night, we are not justified in looking for 8.5 or $\sim$17 hr periods. On timescales below $\sim$5 hr, however, Figures 7 and 8 certainly do not show any obvious short periodicity, although more data will be required to check this, for absolute certainty.

Can the observed line variations be temporally and spatially coherent—created by features of photospheric origin (NRP; CIR)? Emission lines reflect the physical behavior simultaneously in the *whole* wind, except for a cylinder behind the star. Any feature generated in the wind and rotating around the star should produce wavelike variations in velocity space. Such features could move from blue to red, and sometimes vice versa, right across the line center. Because we only observed features moving *away* from the line center in ζ Pup, we assert that the substructures likely represent the stochastic manifestation of turbulent clumps propagating outward with the wind, much the same as already seen in a significant number of W-R star winds.

3.2. *Large-Scale Variations*

In Figure 9 we superpose the mean profiles from each of the two nights. It is quite remarkable that the emission part of the *mean* profile shows very little change over the 2 day interval. This is likely a consequence of the stochastic nature of the clumps. On the other hand, the near-central absorption dip exhibits a clear global decrease over the 2 days, with $\triangle I/I_c \sim 0.03$. This systematic variation is significantly larger than the *mean* variation caused by clumps. Such long-term behavior of He II 4686 is very similar to what is seen in Hα (constant emission, slowly varying near-central absorption) in ζ Pup by Moffat & Michaud (1981). It remains to be seen whether the He II 4686 central absorption follows the rotation period of $P \sim 5.1$ days, as seen in the Hα central absorption.

4. CONCLUSIONS

The wind of ζ Pup shows spectral substructures that are similar to those seen in the winds of W-R stars, which are probably the descendants of O and Of stars. These substructures are likely the consequence of excess emission from clumps caused by supersonic compressible turbulence in the wind. These observations lead naturally to the important question of whether, in fact, all winds in hot stars show such turbulence at one level or another. We note the following for He II 4686 in ζ Pup:

1. As the substructures accelerate toward the blue/red wing of the line, they tend to smear out. Their velocity width is larger when looking along the line of sight. Both of these are observed in W-R spectral lines.
2. The variation profile across the line, $\sigma(\lambda)$, follows the emission-line profile itself, with $\sigma(\lambda)/I(\lambda) \sim 5\%$ and some increase in $\sigma(\lambda)$ on the blue side, as seen in W-R lines (Robert 1992). This is compatible with the whole wind being affected by stochastic variations.
3. Tracing individual substructures and comparison with the standard β velocity law yields $\beta \sim 1.0$–1.2, which is somewhat larger than the standard value for OB winds ($\beta = 0.8$).
4. Using a standard β velocity law for ζ Pup with an adopted stellar radius $R_* = 18\ R_\odot$ (Kudritzki, Simon, & Hamann, 1983) and a terminal velocity of $v_\infty = 2250$ km s^{-1} (Puls et al. 1996), all blobs in He II 4686 appear near the star's surface and disappear at $\sim 2R_*$.
5. The near-central absorption component apparently varies slowly on a nightly basis, much like that seen previously for ζ Pup in Hα (Moffat & Michaud 1981), with $P \approx 5$ days. This variation is likely coupled to the stellar rotation.

Recently, Puls et al. (1996) presented a new method for determining mass loss rates of O stars from Hα line profiles using non-LTE techniques, along with the β-law *Ansatz* for the wind velocity. For ζ Pup their calculations yield $\beta = 1.15$, which is in very good agreement with our observations. They state that "the wind emission contribution to Hα for O stars comes from lower wind layers, typically between 1.0 and 1.5 stellar radii. Very recent hydrodynamical simulations for self-excited wind instabilities show that these layers are unaffected by shocks and that instabilities only occur further out in the wind." However, in ζ Pup we have observed clumping in the He II 4686 line at radii *below* $R \sim 1.5 R_*$. Hence, we presume that the Hα line is also affected by clumping. This would thus imply that mass loss rates of ζ Pup (and possibly of all O stars) calculated from the Hα line profile are overestimated because of the density-squared dependence of recombination emission, as in W-R winds (Moffat & Robert 1994).

The authors would like to thank Grant Hill for making available the Reticon reduction package and Jean-François Bertrand for help in Fortran programming. T. E. is grateful for full financial aid from the Evangelisches Studienwerk, Germany, which is supported by the German Government. S. L. acknowledges support from NSERC (Canada) for a doctoral scholarship. A. F. J. M. thanks NSERC (Canada) and FCAR (Quebec) for financial assistance.

REFERENCES

Baade, D. 1986, in Proc. NATO Workshop, Seismology of the Sun & the Distant Stars, ed. D. O. Gough (Dordrecht: Reidel), 465
———. 1988, in O Stars and Wolf-Rayet Stars, ed. P. S. Conti & A. B. Underhill (Washington, DC: NASA), 137
———. 1991, in ESO Conf. and Workshop Proc. 36, Rapid Variability of OB Stars: Nature and Diagnostic Value, ed. D. Baade (Garching: ESO), 21
Berghöfer, T. W., Baade, D., Schmitt, J. H. M. M., Kudritzki, R.-P., Puls, J., Hillier, D. J., & Pauldrach, A. W. A. 1996a, A&A, 306, 899
Berghöfer, T. W., Schmitt, J. H. M. M., & Cassinelli, J. P. 1996b, A&AS, 118, 481
Blaauw, A. 1993, ASP Conf. Proc. 35, Massive Stars: Their Lives in the Interstellar Medium, ed. J. P. Cassinelli & E. B. Churchwell (San Francisco: ASP), 207
Bohannan, B., Abbott, D. C., Voels, S. A., & Hummer, D. G. 1986, ApJ, 308, 728
Chiueh, T. 1997, ApJ, 482, L179
Chlebowski, T., Harnder, F. R., & Sciortino, S. 1989, ApJ, 341, 427
Cranmer, S. R., & Owocki, S. P. 1996, ApJ, 462, 469
Ebbets, S. D. 1982, ApJS, 48, 399
Feldmeier, A., Kudritzki, R.-P., Palsa, R., Pauldrach, A. W. A., & Puls, J. 1997, A&A, in press
Glaspey, J. 1991, Canada-France-Hawaii Telescope User's Manual, Version 2.0
Harries, T., & Howarth, I. D. 1996, A&A, 310, 533
Henriksen, R. N. 1994, Ap&SS, 221, 25
Hillier, D. J., Kudritzki, R.-P., Pauldrach, A. W. A., Baade, D., Cassinelli, J. P., Puls, J., & Schmitt, J. H. M. M. 1993, A&A, 276, 128
Howarth, I. D., Prinja, R. K., & Massa, D. 1995, ApJ, 452, L65
Johnson, H. L. 1965, ApJ, 141, 923
Kaper, L., Henrichs, H. F., Nichols, J. S., Snoek, L. C., Volten, H., & Zwarthoed, G. A. A. 1996, A&AS, 116, 257
Kudritzki, R.-P., Simon, K. P., & Hamann, W.-R. 1983, A&A, 118, 245
Moffat, A. F. J., & Michaud, G. 1981, ApJ, 251, 133
Moffat, A. F. J., & Robert, C. 1992, in ASP Conf. Ser. 22, Nonisotropic and Variable Outflows from Stars, ed. L. Drissen, C. Leitherer, & A. Nota (San Francisco: ASP), 203
———. 1994, ApJ 421, 310
Owocki, S. P. 1994, Ap&SS, 221, 3
Pauldrach, A. W. A., Puls, J., & Kudritzki, R.-P. 1986, A&A, 164, 86
Prinja, R. K. 1988, MNRAS, 231, 21
———. 1992, in ASP Conf. Ser. 22, Nonisotropic and Variable Outflows from Stars, ed. L. Drissen, C. Leitherer, & A. Nota, 167
Prinja, R. K., & Howarth, I. D. 1986, ApJS, 61, 357
Puls, J., et al. 1996, A&A, 305, 171
Reid, A. H. N., & Howarth, I. D. 1996, A&A, 311, 616
Robert, C. 1992, Ph.D. thesis, Université de Montréal
Schaerer, D., Schmutz, W., & Grenon, M. 1997, ApJ, 484, L153
van der Hucht, K. A., et al. 1997, New Astronomy, 2, 245
Walborn, N. R. 1972, AJ, 77, 312